Generation of Storable Retinal Organoids and Retinal Pigmented Epithelium from Adherent Human iPS Cells in Xeno-Free and Feeder-Free Conditions

Sacha Reichman, Amélie Slembrouck, Giuliana Gagliardi, Antoine Chaffiol, Angélique Terray, Céline Nanteau, Anais Potey, Morgane Belle, Oriane Rabesandratana, Jens Duebel, et al.

Running head title: iPS-derived retinal cells generation and storage

Generation of storable retinal organoids and retinal pigmented epithelium from adherent human iPS cells in xeno-free and feeder-free conditions

Sacha Reichman[1], Amélie Slembrouck[1], Giuliana Gagliardi[1], Antoine Chaffiol[1], Angélique Terray[1], Céline Nanteau[1], Anais Potey[1], Morgane Belle[1], Oriane Rabesandratana[1], Jens Duebel[1], Gael Orieux[1], Emeline F. Nandrot[1], José-Alain Sahel[1,2] and Olivier Goureau[1]

[1]Institut de la Vision, Sorbonne Universités, UPMC Univ Paris 06, INSERM, CNRS UMR 7210, Paris, France

[2]Centre Hospitalier National d'Ophtalmologie des Quinze-Vingts, INSERM-DHOS CIC 1423, Paris, France

AUTHOR CONTRIBUTION

Sacha Reichman: Conception and design, collection and/or assembly of data, data analysis and interpretation, manuscript writing, final approval of manuscript

Amélie Slembrouck: Conception and design, collection and/or assembly of data, data analysis and interpretation, final approval of manuscript

Giuliana Gagliardi: Collection and/or assembly of data, data analysis and interpretation, manuscript writing, final approval of manuscript

Antoine Chaffiol: Collection and/or assembly of data, data analysis and interpretation, final approval of manuscript

Angélique Terray: Collection and/or assembly of data

Céline Nanteau: Collection and/or assembly of data

Anais Potey: Provision of study material

Morgane Belle: Provision of study material

Oriane Rabesandratana: Provision of study material

Jens Duebel: Provision of study material

Gael Orieux: Provision of study material

Emeline Nandrot: Collection and/or assembly of data, data analysis and interpretation, final approval of manuscript

José-Alain Sahel: Administrative and financial support, final approval of manuscript

Olivier Goureau: Financial support, conception and design, collection and/or assembly of data, data analysis and interpretation, manuscript writing, final approval of manuscript

CONTACT: Olivier Goureau

Institut de la Vision, 17, Rue Moreau 75012 Paris, France

Email: olivier.goureau@inserm.fr

Tel: (33) 1.53.46.25.33 Fax: (33) 1. 44. 53.46.26.00

Abstract

Human induced pluripotent stem cells (hiPSCs) are potentially useful in regenerative therapies for retinal disease. For medical applications, therapeutic retinal cells, such as retinal pigmented epithelial (RPE) cells or photoreceptor precursors, must be generated under completely defined conditions. To this purpose, we have developed a two-step xeno-free / feeder-free (XF/FF) culture system to efficiently differentiate hiPSCs into retinal cells. This simple method, relies only on adherent hiPSCs cultured in chemically defined media, bypassing embryoid body formation. In less than one month, adherent hiPSCs are able to generate self-forming neuroretinal-like structures containing retinal progenitor cells (RPCs). Floating cultures of isolated structures enabled the differentiation of RPCs into all types of retinal cells in a sequential overlapping order, with the generation of transplantation-compatible $CD73^+$ photoreceptor precursors in less than 100 days. Our XF/FF culture conditions allow the maintenance of both mature cones and rods in retinal organoids until 280 days with specific photoreceptor ultrastructures. Moreover, both hiPSC-derived retinal organoids and dissociated retinal cells can be easily cryopreserved while retaining their phenotypic characteristics and the preservation of $CD73^+$ photoreceptor precursors. Concomitantly to neural retina, this process allows the generation of RPE cells that can be effortlessly amplified, passaged and frozen while retaining a proper RPE phenotype. These results demonstrate that simple and efficient retinal differentiation of adherent hiPSCs can be accomplished in XF/FF conditions. This new method is amenable to the development of an *in vitro* GMP-compliant retinal cell manufacturing protocol allowing large-scale production and banking of hiPSC-derived retinal cells and tissues.

Introduction

The impaired or complete loss of function of photoreceptor cells or supporting retinal pigmented epithelium (RPE) is the main cause of irreversible blindness in retinal diseases, such as inherited retinopathies and age-related macular degeneration (AMD). The death of retinal ganglion cells (RGCs) in glaucoma also results in irreversible loss of vision. Cell replacement strategies using cell derivatives of pluripotent stem cells are very promising approaches to rescue the degenerated retina. Stepwise differentiation protocols were designed to mimic retinal differentiation and to successfully generate RPE cells, RGCs and photoreceptors from human embryonic stem cells (hESCs) and induced pluripotent stem cells (hiPSCs) [1–14]. Recent innovative process demonstrated that hESCs or hiPSCs could efficiently form 3D retinal structures, starting from embryoid bodies [15–18] or simply from confluent hiPSC cultures [19, 20]. The majority of these approaches often rely on animal-derived components in the medium and animal-derived substrate or feeder layer. Therefore, the establishment of a defined and completely xeno-free (XF) culture system following current Good Manufacturing Practice (GMP) guidelines for the generation of transplantable retinal cell types derived from hESCs or hiPSCs is needed for future clinical applications. The use of a feeder-free (FF) system with chemically defined media is now well described for the culture hESCs and hiPSCs [21], as well as for the generation of RPE cells [6, 22–24] including from hESCs in clinical conditions [25]. However XF/FF culture conditions are poorly documented for differentiation towards retinal neurons [26, 27].

In the current study, we have developed a new retinal differentiation method of hiPSCs in absence of xenogeneic products, based on our simple method allowing both the self-formation of neural retina-like structures and the generation of RPE cells from confluent hiPSCs [19, 28]. This XF approach is compatible with the cryopreservation of both hiPSC-derived RPE cells and neural retinal cells. We show for the first time the capability of both hiPSC-derived retinal organoids and dissociated retinal cells to be stored while retaining their phenotypic characteristics, needed for their utilization in cell transplantation.

Materials and Methods

Human iPSC cultures

Established hiPSC-2 clone [19], previously cultured on mitomycin inactivated mouse embryonic fibroblasts, was adapted to feeder-free conditions. iPS colonies from hiPSC-2 clone cells were incubated 7 to 10 min in 2 ml of enzyme-free Gentle cell dissociation reagent (STEMCELL Technologies) at room temperature. After aspiration of the dissociation solution, detached cell aggregates were resuspended in 2 ml of pre-warmed chemical defined Essential 8™ medium (Thermo Fischer Scientific) by pipetting up and down the center of the iPS colonies without detaching the feeder cells. Human iPSCs were transferred on truncated recombinant human vitronectin (rhVTN-N)-coated dishes with Essential 8™ medium. Cells were routinely cultured at 37°C in a standard 5% CO_2 / 95% air incubator with a daily medium change. iPS cells were passaged with the enzyme-free Gentle cell dissociation reagent (2 ml for 7 min at room temperature) every week. Detached cell aggregates were collected in Essential 8™ medium and carefully pipetted up and down to obtain uniform suspension of cell aggregates that are replated at ratio of 1/10 to 1/60 depending on the confluence. Feeder free-adapted hiPSCs were subjected to retinal differentiation after 3 to 5 passages. Adapted at passage 16 (p16), the hiPSC-2 clone was used between p20 to p40 for characterization and differentiation.

Retinal differentiation and hiPSC-derived retinal cell cultures

Retinal cell differentiation was based on our previously established protocol [28] with some modifications. Human iPSCs were expanded to 70-80 % confluence in 6-cm diameter dishes coated with rhVTN-N (Thermo Fischer Scientific) in Essential 8™ medium. At this time, defined as day 0 (D0), hiPSCs were cultured in chemical defined Essential 6™ medium (Thermo Fischer Scientific). After 2 days, the medium was switched to E6N2 medium composed of Essential 6™ medium, 1% CTS™ (Cell Therapy Systems) N2 supplement (Thermo Fischer Scientific), 10 units/ml Penicillin and 10 µg/ml Streptomycin (Thermo Fischer Scientific). The medium was changed every 2-3 days. On D28, identified self-formed

retinal organoids were isolated, using a needle, with the surrounding cells and cultured in 6-well-plates (8 to 12 organoids per well) as floating structures in the ProB27 medium supplemented with 10 ng/ml of animal-free recombinant human FGF2 (Peprotech) and half of the medium was changed every 2-3 days. ProB27 medium is composed of chemical defined DMEM:Nutrient Mixture F-12 (DMEM/F12, 1:1, L-Glutamine), 1% MEM non-essential amino acids, 2% CTS™ B27 supplement (Thermo Fischer Scientific), 10 units/ml Penicillin and 10 µg/ml Streptomycin. At D35, FGF2 was removed and half of the "ProB27 medium" was changed every 2-3 days for the next several weeks.

For hiPSC-derived RPE (hiRPE) cell cultures, identified pigmented patches were cut around D42 and transferred, noted as passage 0 (P0), onto plates coated with CTS™ CELLStart™ (Thermo Fischer Scientific). hiRPE cells were expanded in the ProN2 medium composed of DMEM/F12, 1% MEM non-essential amino acids, 1% CTS™ N2 supplement, 10 units/ml Penicillin and 10 µg/ml Streptomycin; and the medium was changed every 2-3 days. At confluence, hiRPE cells were dissociated using trypsin and replated at $5x10^4$ cells/cm² onto T-25 cm² CTS™ CellStart™-coated dishes for amplification before banking.

Cryopreservation of hiPSC-derived retinal cells

Three to five retinal organoids at D84 were suspended in 250 µl of cold Cryostem freezing medium (Clinisciences) and frozen in a 1.5 ml cryogenic tube (Nunc) placed in isopropanol-based Mr Frosty freezing container (Thermo Fischer Scientific) at -80°C for a minimum of 4 hours. Frozen tubes were kept in a -150°C freezer for long-term storage. HiRPE cells were frozen at passage 1 in Cryostem freezing medium ($1.5x10^6$ cells/ 250 µl) using the same method with the freezing container and were placed at -150°C for long-term storage. Frozen retinal structures or hiRPEp1 cells were thawed quickly at 37°C in a water bath and resuspended in prewarmed dedicated media for downstream investigations.

Retinal organoid immunostaining-clearing and imaging

Retinal organoids were first incubated at RT on a rotating shaker in a solution (PBSGT) of PBS 1X containing 0.2% gelatin, 0.5% Triton X-100 and 0.01% thimerosal (Sigma-Aldrich) for 3 hr. Samples were next transferred to PBSGT containing the selected primary antibodies (Table S1) and placed at 37°C for 3 days, with rotation at 100 rpm. This was followed by six washes for 30 min in PBSGT at RT. Next, samples were incubated with appropriate secondary antibodies conjugated with either Cy3 or Alexa Fluor 594 (Interchim) diluted at 1:600 in PBSGT overnight. After six 30-min washes in PBSGT at RT, samples were stored at 4°C in PBS until the 3D imaging of solvent-cleared organ (3DISCO) clearing procedure [29]. Samples were first dehydrated in a graded series (50%, 80% and 100%) of tetrahydroflurane (Sigma-Aldrich) diluted in H_2O, during 1hr for each step. This was followed by a delipidation in dichloromethane (Sigma-Aldrich) for at least 20 min, and finally, samples were cleared overnight in dibenzylether (Sigma-Aldrich). 3D imaging was performed either with an ultramicroscope (LaVision BioTec) using the ImspectorPro software (LaVision BioTec) or an upright confocal microscope (Olympus FV1000) with a numerical 10X objective for high-resolution imaging, as previously described [29]. Images, 3D volume and movies were generated using Imaris x64 software (version 7.6.1, Bitplane) using the “snapshot” and “animation” tools. Movie legends were generated using iMovie 10.0.2.

Results

Generation of self-forming retinal organoids in Xeno-Free / Feeder-Free conditions from confluent hiPSCs

Human iPSC colonies from the integration-free iPS cell line 2 (hiPSC-2), previously generated by episomal approach [19], were adapted to XF/FF culture system using the truncated recombinant human vitronectin (rhVTN-N) as synthetic substrate and chemical defined Essential 8^{TM} medium [21]. Under these new conditions, qRT-PCR revealed that the expression of pluripotency genes in hiPSC-2 is still comparable to that seen in hESCs (Figure S1A). hiPSC-2 expanded in XF/FF conditions express the pluripotency markers

OCT4 and SSEA4 or SOX2 and TRA1-60 (Figure S1B-G) and exhibited a normal karyotype (Figure S1H).

At around 70% of confluence, hiPSC colonies cultured in Essential 8™ medium were placed in Essential 6™ medium (Essential 8™ medium without FGF2 and TGFß) during 2 days to turn off the self-renewal machinery and encourage the spontaneous differentiation. Since we previously reported that N2 supplement alone could be sufficient to direct hiPSCs cultured on feeder layers toward retinal fate [19], we tested different chemically defined media containing 1% of CTS™ N2 supplement (Figure 1A). In this XF/FF environment, the use of ProN2 medium validated with hiPSCs on feeder layers [19] led regretfully to cell death (data not shown). Nevertheless, we developed a new retinal differentiation medium (E6N2 medium), corresponding to Essential 6™ medium containing 1% of CTS™ N2 supplement, allowing the self formation of neuroepithelial-like structures from adherent hiPSCs in 28 days (Figure 1A). In this XF/FF conditions, differentiating iPSCs started within 14 days (D14) to endogenously express the key BMP and WNT antagonists, DKK1 and NOGGIN respectively, essential for neural differentiation (Figure 1B). About four weeks after the initiation of differentiation, self-forming neuroepithelial-like structures appeared in the culture dishes (Figure 1C and Figure S2A). RT-qPCR analysis of these isolated structures at D28 (Figure 1D) revealed an eye-field specification with the robust expression of specific markers, such as *SIX3, MITF, VSX2, PAX6, RAX* and *LHX2*, while losing the expression of the pluripotency marker *POU5F1 (OCT4)* (Figure 1E). Immunostaining at D28 showed that these structures comprise a population of mitotic retinal progenitor cells (RPCs) coexpressing VSX2 and Ki67 (Figure 4A). The expression of transcription factors involved in the photoreceptor lineage, such as *CRX*, *NRL* and *NEUROD1*, was also detected as early as D28 (Figure 1E).

Following isolation along with surrounding cells at D28, retinal organoids were cultured as floating structures (Figure 1D and Figure S2B) in medium containing CTS™ B27 supplement (ProB27 medium) with human FGF2 during 1 week (Figure 1A) to favor differentiation of the neural retina [30]. Spherical organoids increased in size and the distal part of the neuroepithelium became pigmented around D42 (Figure S2B-D). To confirm the

reproducibility of the differentiation process, two other hiPSC lines were subjected to the XF/FF differentiation process. Our results demonstrated that similar retinal organoids can be obtained indifferently from hiPSCs derived from foreskin fibroblasts reprogrammed by an episomal approach (Figure S2E-F) or derived from adult dermal fibroblasts reprogrammed in XF/FF conditions with the Sendai virus (Figure S2G-H). The evaluation of the number of structures that developed per cm² for these three hiPSC lines at D28 revealed some expected inter-cell line variability in term of efficiency (Figure S2I).

Transcription factors involved in retinal specification and differentiation were still expressed in retinal organoids during floating cultures in ProB27 medium, with a noticeable increase of *RAX*, *SIX3* and *VSX2* expression after D35, while expression of the non-retinal forebrain marker *FOXG1* decreased (Figure 1F). At D35, cells forming retinal organoids co-expressed RAX and PAX6 (Figure 1H and 1I) confirming their eye-field identity [31]. At this time, $VSX2^{+}$ cells were predominantly located in the outer part of the developing neuroepithelium (Figure 1J-L), which also expressed also PAX6 (Figure 1J and 1K). $MITF^{+}$ cells were found mainly in the distal part of the organoids (Figure 1L and 1M), corresponding to RPE cells. At D35, the $PAX6^{+}/VSX2^{-}$ cell population is concentrated at the inner part of neuroepithelium (Figure 1J and 1K), corresponding to the first post-mitotic differentiating retinal neurons, which did not express the Ki67 proliferation marker (Figure 1N and 1O). Some cells in the same location were found to be immunoreactive for a specific marker of RGCs, BRN3A (Figure 4B). Nevertheless, at D35, the outer part of retinal organoids still contained proliferative RPCs identified by the co-expression of VSX2 and Ki67 (Figure 1O). Interestingly, RT-qPCR analysis showed that the emergence of photoreceptor precursors can be detected after D42 by up-regulation of *NRL*, *CRX* and *NEUROD1* expression (Figure 1G), concomitant to the decrease of *VSX2* and *RAX* expression (Figure 1F).

Differentiation of RPCs from hiPSC-derived retinal organoids

RT-qPCR analysis on organoid RNA extracts showed that RPCs can be committed in to the photoreceptor lineage, with an increase of *CRX* (Figure 1G), *RECOVERIN* (*RCVRN*) and

CONE ARRESTIN (*CAR*) expression (Figure 2A) throughout the floating culture. The expression of genes specific for mature photoreceptors, such as *RHODOPSIN* (*RHO*), *BLUE* or *RED/GREEN* (*R/G*) *OPSIN* (*OPS*), emerges only after 100 days (Figure 2B). Immature photoreceptors immunoreactive for CRX, OTX2, and RCVRN can be identified at D49 (Figure 2C and 2D), and a stronger expression of these markers was observed at D84 (Figure 2E). Rods and cones can be clearly identified either by RHO or R/G OPS, BLUE OPS and CAR immunostaining in culture kept for a longer period until D281 (around 9 months) (Figure 2G-N). Interestingly, after 40-50 days, differentiating photoreceptors were often found inside rosettes (Figure 2C-G), even though an external cell layer resembling the outer nuclear layer can be observed in some iPSC-derived retinal organoids (Figure 2H, I and Figure S3C). The cell surface marker CD73 is expressed specifically in differentiating $RCVRN^+$ photoreceptors at different times of differentiation (Figure 2D, F and Figure S3B). The expression of CD73 by photoreceptors was confirmed after D140 by the co-expression with RCVRN, CAR, BLUE OPS and R/G OPS (Figure 2J and Figure S3). Conversely, CD73 was not expressed by $PAX6^+$ cells (corresponding to RGCs and horizontal/amacrine cells) located around the rosettes (Figure S3A). An efficient photoreceptor differentiation was also observed in retinal organoids derived from the two other hiPSC lines showing cells expressing RCVRN, CAR, CRX, RHO, BLUE OPS and R/G OPS between D77 and D175 (Figure S4). In 175-days old retinal organoids, the connecting cilium marker acetylated TUBULIN revealed the existence of very thin structures juxtaposed to $RCVRN^+$ cells (Figure 2I), suggesting the formation of cilia and photoreceptor outer segments (POS).

To analyze the spatial distribution of rosettes containing rods and cones, we performed whole-mount immunostaining with photoreceptor specific markers and 3DISCO clearing procedure on D195 retinal organoids. This technology offers the possibility of imaging entire transparent samples without the need of sectioning, when combined with immunohistochemistry [29]. Spatial arrangement of photoreceptors characterized by the expression of RCVRN/RHO and CAR/RHO was observed on 3D-reconstructed images (Figure 3A, B). The precise 3D pattern of rosettes containing RHO^+ rods or CAR^+ cones was

visualized in the external part of the retinal organoids (Figure 3C and Movies S1 and S2). High-resolution confocal imaging of RHO staining on cleared D195 organoids revealed an intense fusiform staining reminiscent of emerging POS in the center of rosettes (Figure 3D). Similar staining was observed with CAR antibody identifying cones in different retinal organoids (Figure S4J). TUNEL assay performed on 195-days old organoids demonstrated that photoreceptors identified by RCVRN, RHO or BLUE OPS staining in the rosettes do not seem to undergo apoptosis (Figure S5). Transmission electronic microscopy analysis confirmed the presence of photoreceptor ultra structures, such as basal body and connecting cilium with a photoreceptor-specific microtubule arrangement at D112 (Figure 3E-3K). Some photoreceptors also presented membranous materials, corresponding to developing POS, which were clearly identified at D196 (Figure 3L).

To test whether the hiPSC-derived photoreceptors are capable of achieving functional maturation, we tested their ability to exhibit an inward dark current (IDC). The IDC corresponding to an influx of Na^+ and Ca^{2+} through the activation of cyclic nucleotide-gated (CNG) channels is the result of the increase of the cGMP concentration in photoreceptors. To mimic this "dark state", we used a membrane-permeant cGMP analogue (8-Br-cGMP) to open cationic CNG channels leading to the IDC, as previously described [18]. Ca^{2+} influx was monitored with live two-photon imaging of the intracellular fluorescent Ca^{2+} indicator Fura-2 in dissociated cells from retinal organoids at D175. Forty-eight hours after seeding, some Fura-2-loaded retinal cells showed a calcium influx when exposed to 8-Br-cGMP, as observed by decreased intracellular fluorescence (Figure 3M-N). Average of maximum fluorescence variation during recording of 11 responsive photoreceptors is -22.52 +/- 10.63 % (151 cells analyzed, *N*=4) (Figure 3O). No decrease of the intracellular fluorescence has been observed in retinal cells exposed to AMES puffs instead of the cGMP analogue (150 cells analyzed, *N*=4). These functional observations support our morphological data that the XF/FF culture conditions reported here allow a certain level of photoreceptor maturation.

The RPCs within retinal organoids are able to give rise to other retinal cell types. By RT-qPCR and immunostaining using BRN3 markers, we confirmed the early emergence of the

RGCs after 35 days of differentiation (Figure 4C and 4K). Interestingly, BRN3A$^+$ RGCs localized around the rosettes containing OTX2$^+$ photoreceptors can still be observed in 84-days old organoids when ProB27 medium was used (Figure 4F). Similar immunofluoresence analysis confirmed the differentiation of RGCs in retinal organoids derived from the two other hiPSC lines (Figure S4A-C and S4E), confirming the reproducibility of the differentiation process. Differentiating amacrine and horizontal cells were detected by RT-qPCR with the induction of *GAD2* and *LIM* expression respectively (Figure 4L) and by immunohistochemistry with the presence of AP2$^+$/PAX6$^+$ and LIM1$^+$/PAX6$^+$ cells respectively (Figure 4D and 4E). RT-qPCR demonstrated that bipolar cells identified by PKCα expression appear later (Figure 4M) and immunostaining at D281 confirmed the presence of fully differentiated bipolar cells co-expressing VSX2 and PKCα (Figure 4I, J). The emergence of Müller glial cells was also observed at later time points, as shown by RT-qPCR with the induction of specific markers *GLAST1* and *RLBP1* (Figure 4M) and by the identification of cells co-expressing the GLUTAMINE SYNTHETASE (GS) and SOX9 (Figure 4G). At D140, the presence of very rare Ki67$^+$ cells (less than 5 positive cells per section) indicates that retinal organoids reached a “mature state”, confirmed by the absence of mitotic RPCs (Figure 4H).

Cryopreservation of photoreceptor precursors from retinal organoids

Considering the potential use of photoreceptor precursors for future cell transplantation [32, 33] and the length of the differentiation, we sought to develop different cryopreservation approaches that would enable the cells to be stored along the differentiation process. The first strategy was to cryopreserve whole retinal organoids at stages of development where CD73 is well expressed (close to D100, as shown by immunofluorescence). Retinal organoids cultured in suspension until D84 were submitted to cryopreservation using cold Cryostem® freezing medium and the presence of photoreceptors was examined in organoids 16 days after thawing, at D100, in floating cultures. Frozen retinal organoids showed the presence of intact rosettes containing CRX$^+$ and RCVRN$^+$ photoreceptor precursors (Figure

5E, F) similar to non-frozen organoids at the same stage (Figure 5A, B). Interestingly, the CD73$^+$ cells, considered as the transplantable cell population [34–36], were still clearly identified. Indeed, as in non-frozen organoids (Figure 5C, D), CD73 is specifically expressed in RCVRN$^+$ cells (Figure 5G, H) confirming their specific expression in photoreceptors. Quantification of CRX$^+$ cells at D100 (Figure 5Q) did not reveal any significant difference between the number of cells in controls (non frozen) and frozen retinal organoids (p=0.1344; n=81,450 and 119,339 counted cells).

In a second approach, we examined whether dissociated retinal cells from organoids could be cryopreserved. In this case, retinal organoids cultured until D84 or D100 were dissociated using papain and retinal cells were cryopreserved using the cold Cryostem® freezing medium. After thawing, cells were plated on Poly-D-Lysin / Laminin treated coverslips to be cultured for 5 additional days in vitro (DIV). Immunostaining revealed that frozen RCVRN$^+$ photoreceptors have kept their strong CD73 expression as in non frozen dissociated cells (Figure 5I-L). Similar observations were made on a double CRX$^+$ and RCVRN$^+$ cell population (Figure 5M-P). Accordingly, quantification showed no significant difference in the number of double CRX$^+$ and RCVRN$^+$ cells was observed between frozen cells and control cells (Figure 5R) (p=0.5839; n=31,303 and 23,958 counted cells).

Generation, amplification and banking of hiPSC-derived RPE cells.

Human iPS-derived RPE (hiRPE) cells were generated simultaneously to the retinal organoids from confluent hiPSCs cultured in Essential 6^{TM} medium with the successive addition after 2 days of the CTS^{TM} N2 supplement until D28 (Figure 6A). After removal of self-forming retinal organoids, cell cultures were switched to ProN2 medium. Around D42, pigmented patches of cells were picked up and hiRPE cells were amplified from these patches (Figure 6B, C). After 2 weeks, hiRPE cells at passage 1 (hiRPEp1) were cryopreserved for cell banking and thawed hiRPE cells at passage 3 (hiRPEp3) were used for complete characterization (Figure 6D, E). Generated epithelial cells were immunoreactive for the key RPE-specific transcription factor MITF and the tight junction marker ZO-1 (Figure

6F). Counting the number of $MITF^+$ cells confirmed the purity of the cell culture with 99.83 ± 0.31 % of positive cells (n=208,259 cells). Immunostaining for BESTROPHIN (BEST1) and EZRIN showed a correct polarization of hiRPE cells in culture with the expression of these proteins at the basolateral membrane and the apical side of the cells respectively (Figure 6G, H). RT-qPCR analysis also demonstrates that cells retained the expression of mature RPE-associated markers such as *PEDF, VEGF, MERTK* and *BEST1* after freezing and at least for 3 additional passages (Figure 6I). Long-term cultures of hiRPEp3 cells depicted a closer RPE phenotype to human primary cultures, particularly for *RPE65*, which is strongly expressed in adult human RPE cells (Figure 6J). We investigated whether hiRPE cells after banking still exhibited typical native RPE functions. Using ELISA we showed vascular endothelial growth factor (VEGF) and pigment epithelium derived factor (PEDF) secretion by hiRPEp3 cells with respective values of 12.4+0.5 ng/ml and 80.5+8.8 ng/ml (*n*=3). We also demonstrated the ability of hiRPEp3 cells to carry out specific phagocytosis of FITC-labeled POS similarly to the human immortalized RPE cell line ARPE-19 (Figure 6K-Q). Conversely to fibroblasts, POS phagocytosis by both hiRPE and ARPE-19 cells was blocked by an antibody against integrin $\alpha v\beta 5$, demonstrating the specificity of POS phagocytosis linked to this receptor by RPE cells, as previously demonstrated [37, 38].

Discussion

In the current study, we propose a new protocol to generate retinal organoids and RPE cells from adherent hiPSCs using a defined XF/FF culture system amenable to future clinical grade production. To keep simple a protocol avoiding EB formation and the use of substrates such as Matrigel as previously described in xenogeneic condition [19, 28], retinal differentiation in the XF/FF culture conditions has required the assessment of critical points. We have determined the right time-point to start the differentiation of adherent hiPSCs, developed new chemical defined differentiation medium and established the optimal timing to collect emerging retinal organoids. The replacement of feeders by human vitronectin, which supported pluripotency of hESCs and hiPSCs in a XF defined medium [21], enables the

generation of self-forming neuroretinal structures and RPE cells, when expanded iPSC colonies were placed in successive chemically-defined proneural media with animal-free CTS™ supplements (ThermoFischer Scientific). The endogenous production by hiPSCs of DKK1 and NOGGIN, two inducers of neural and retinal specification, could explain the self-formation of these structures, as previously reported [19]. The presence of recombinant human Insulin in the CTS™ N2 supplement, could play a similar role to that of IGF-1, generally added to promote the retinal lineage [9, 12]. Isolated structures cultured as floating retinal organoids in ProB27 medium allowed the differentiation of multipotent RPCs in all the retinal cell types in a sequential overlapping order, similar to the one we previously reported in xenogeneic conditions [19]. RGCs were detected as early as D35 followed by horizontal and amacrine cells, whereas mature photoreceptors, expressing OPSIN or RHODOPSIN, and bipolar or Müller glial cells were clearly identified after a D100. Interestingly, our culture conditions allowed the maintenance of both mature S and L/M cones and rods in retinal organoids until D281 (>9 months). The presence of a specific PR ultrastructures confirms that our XF/FF conditions permit the maturation of photoreceptors with similar structures to those observed in the developing human retina [39]. Further evidence of the advanced level of maturation is the sensitivity of a proportion of hiPSC-derived photoreceptors to cGMP stimulation in a similar manner to native photoreceptors. Moreover, we demonstrated that adaptation of the tissue clearing procedure 3DISCO [29] to retinal organoids, allowed the analysis of fluorescently labeled retinal cells in transparent organoids while preserving original shape and structure. This approach provides a global view of retinal cell type development, spatial arrangement and connections within the organoids. When combined with high-resolution microscopy, this technique could be used for a rapid and efficient analysis of normal and pathological features in intact retinal organoids generated from patient-specific iPSCs.

For future cell therapy strategies based on purified photoreceptor precursors, our XF/FF protocol allows, in less than 100 days, the generation of CD73-positive photoreceptor precursors, described as a transplantation-compatible cell population in mouse [34–36]. We

have demonstrated that CD73 is a marker of photoreceptor precursors and continues to be expressed in differentiated photoreceptors, particularly cones expressing R/G or BLUE OPSIN, in contrast to mice where rare BLUE OPSIN cones do not express CD73 [40]. Since the transplantation in ONL-degenerated host retinas should also be considered, the intact neuroretinal tissue of the retinal organoids derived from hiPSCs in XF/FF conditions could be of clinical utility, as recently proposed for hESC-derived retinal tissues [41]. In this context of retinal sheet transplantation, the ontogenic stages of differentiated tissues from hESCs or hiPSCs should be clearly defined for successful transplantation. Nevertheless, a therapeutic translation of these cells would require a constant production in terms of cell quantity and consistency that it is not likely to be achieved with a fresh cell therapy product (CTP). Therefore, developing an adequate cryopreservation of the CTP is a crucial aspect to ensure a continual delivery of the cell population of interest. Cryopreservation of the whole retinal organoids demonstrated that in frozen-thawed structures the $CD73^+$ photoreceptor precursor population is preserved. This should make it possible to prepare large-scale stocks of retinal organoids at specific stages to deliver pure transplantation-competent $CD73^+$ cells when needed. Furthermore, our freezing method enables the cryopreservation of dissociated retinal cells including photoreceptor precursors without loss of membrane expression of CD73. This observation highlights the alternative possibility of using thawed dissociated retinal cells and potentially a thawed and homogenous population of $CD73^+$ cells for cell transplantation. However, it will be important to determine what kind of cryopreservation process and purification method induces less cell stress and would be the most effective for subretinal grafting.

In addition to photoreceptor precursors, the production of hiPSC-derived RGCs in our XF/FF conditions could have important implications for the treatment of retinal dystrophies affecting the RGCs such as glaucoma. The fast emergence of RGCs in organoids and the use of CTS™ B27-containing medium that keeps them alive longer compared to N2-containing medium [19], should facilitate the development of cell-based therapy approaches using hiPSC-derived RGCs. Our cryopreservation technique would be useful to freeze retinal

organoids at relatively early stages (before day 50) to make frozen stocks of RGC precursors that could be deliver when needed.

Concomitantly to the neural retina, our protocol allows the generation of RPE cells from hiPSCs that can be easily amplified, passaged and frozen while retaining a proper RPE phenotype and RPE specific functions such as POS phagocytosis and trophic factor secretion. Gene expression assays indicated that hiRPE cell maturation could be achieved by extending the length of culture time. Large-scale production of hiRPE cells can be reached with our XF/FF conditions, since one 6-cm² dish can produce up to 500 millions of hiRPE cells after 3 passages. Based on previous reports, using either hESC-derived RPE cells in suspension [25] or sheets of hiPSC-derived RPE cells [42], we believe that the XF/FF differentiation protocol reported here could deliver sufficient quantities of cells to perform several thousands of injections. A large-scale production of these cells could be required with the future development of global haplotype hiPSC banking, where a limited number of cell lines with common HLA haplotypes will be derived in order to match a significant portion of the patient population [43, 44].

Conclusion

The present study shows that simple and efficient retinal differentiation of adherent hiPSCs can be accomplished in XF/FF environment near to clinical conditions with the use of minimal and GMP-compatible raw materials. This new method is amenable to the development of an *in vitro* GMP-compliant retinal cell manufacturing protocol allowing for large-scale production and banking of hiPSC-derived retinal cells and tissues. Human iPSCs used in this study have been generated by a non-integrative approach, thus addressing one major limitation for future clinical applications of hiPSCs generated from integrative delivery systems. Considering these advances, future cell therapy requiring transplantation of RGCs, photoreceptors or RPE cells to treat retinal degeneration could be achieved.

Acknowledgements

We are grateful to G. Toutirais (Electronic microcopy facility, UPMC-Paris 6) for performing TEM analysis, Dr. C. Craft (Mary D. Allen Laboratory for Vision Research, USC ROSKI Eye Institute) for cone arrestin antibody and Dr. M. Garita-Hernandez for critical reading. We thank S. Fouquet and D. Godefroy from the imaging facility and M. Lechuga from the automated high content analysis platform, both supported by "Département de Paris and by Région Ile de France" and Dr. N. Oudrhiri and Prof. A. Bennaceur, (Service d'hématologie cytogénétique GHU Paris-Sud APHP, INGESTEM ANR Programme Investissements d'Avenir) for the conventional cytogenetic analysis. This work was supported by grants from the Agence Nationale de la Recherche (ANR) [GPiPS: ANR-2010-RFCS005], the Accelerating Technology Transfer SATT Lutech (CelliPSight), the "Fondation pour la Recherche Médicale" (Bio-engineering program - DBS20140930777) and the Retina France association to O.G. This work was also performed in the frame of the LABEX LIFESENSES [ANR-10-LABX-65] supported by the ANR within the Programme Investissements d'Avenir [ANR-11-IDEX-0004-02]. A.T. was supported by a grant from the Fondation de France (Berthe Fouassier) and O.R. from the Fédération des Aveugles et des Handicapés Visuels de France.

Disclosure of Potential Conflicts of Interest

The authors indicate no potential conflicts of interest

References

1. Osakada F, Ikeda H, Mandai M, et al. Toward the generation of rod and cone photoreceptors from mouse, monkey and human embryonic stem cells. Nat. Biotechnol. 2008;26(2):215–24.
2. Idelson M, Alper R, Obolensky A, et al. Directed differentiation of human embryonic stem cells into functional retinal pigment epithelium cells. Cell Stem Cell 2009;5(4):396–408.
3. Krohne TU, Westenskow PD, Kurihara T, et al. Generation of retinal pigment epithelial cells from small molecules and OCT4 reprogrammed human induced pluripotent stem

cells. Stem Cells Transl. Med. 2012;1(2):96–109.

4. Kokkinaki M, Sahibzada N, Golestaneh N. Human induced pluripotent stem-derived retinal pigment epithelium (RPE) cells exhibit ion transport, membrane potential, polarized vascular endothelial growth factor secretion, and gene expression pattern similar to native RPE. Stem Cells 2011;29(5):825–35.
5. Zahabi A, Shahbazi E, Ahmadieh H, et al. A new efficient protocol for directed differentiation of retinal pigmented epithelial cells from normal and retinal disease induced pluripotent stem cells. Stem Cells Dev. 2012;21(12):2262–72.
6. Buchholz DE, Pennington BO, Croze RH, et al. Rapid and efficient directed differentiation of human pluripotent stem cells into retinal pigmented epithelium. Stem Cells Transl. Med. 2013;2(5):384–93.
7. Maruotti J, Wahlin K, Gorrell D, et al. A simple and scalable process for the differentiation of retinal pigment epithelium from human pluripotent stem cells. Stem Cells Transl. Med. 2013;2(5):341–54.
8. Meyer JS, Shearer RL, Capowski EE, et al. Modeling early retinal development with human embryonic and induced pluripotent stem cells. Proc. Natl. Acad. Sci. U. S. A. 2009;106(39):16698–703.
9. Zhu Y, Carido M, Meinhardt A, et al. Three-dimensional neuroepithelial culture from human embryonic stem cells and its use for quantitative conversion to retinal pigment epithelium. PLoS One 2013;8(1):e54552.
10. Zhou S, Flamier A, Abdouh M, et al. Differentiation of human embryonic stem cells into cone photoreceptors through simultaneous inhibition of BMP, TGFβ and Wnt signaling. Development 2015;142(19):3294–306.
11. Yanai A, Laver CRJ, Joe AW, et al. Differentiation of human embryonic stem cells using size-controlled embryoid bodies and negative cell selection in the production of photoreceptor precursor cells. Tissue Eng. Part C. Methods 2013;19(10):755–64.
12. Lamba DA, Karl MO, Ware CB, et al. Efficient generation of retinal progenitor cells from human embryonic stem cells. Proc. Natl. Acad. Sci. U. S. A. 2006;103(34):12769–74.

13. Tucker BA, Mullins RF, Streb LM, et al. Patient-specific iPSC-derived photoreceptor precursor cells as a means to investigate retinitis pigmentosa. Elife 2013;2:e00824.
14. Mellough CB, Sernagor E, Moreno-Gimeno I, et al. Efficient stage-specific differentiation of human pluripotent stem cells toward retinal photoreceptor cells. Stem Cells 2012;30(4):673–86.
15. Meyer JS, Howden SE, Wallace KA, et al. Optic vesicle-like structures derived from human pluripotent stem cells facilitate a customized approach to retinal disease treatment. Stem Cells 2011;29:1206–1218.
16. Nakano T, Ando S, Takata N, et al. Self-formation of optic cups and storable stratified neural retina from human ESCs. Cell Stem Cell 2012;10(6):771–85.
17. Zhong X, Gutierrez C, Xue T, et al. Generation of three-dimensional retinal tissue with functional photoreceptors from human iPSCs. Nat. Commun. 2014;5(May):4047.
18. Mellough CB, Collin J, Khazim M, et al. IGF-1 Signalling Plays an Important Role in the Formation of Three Dimensional Laminated Neural Retina and Other Ocular Structures from Human Embryonic Stem Cells. Stem Cells 2015;33(8):2416-30.
19. Reichman S, Terray A, Slembrouck A, et al. From confluent human iPS cells to self-forming neural retina and retinal pigmented epithelium. Proc. Natl. Acad. Sci. U. S. A. 2014;111(23):8518–23.
20. Singh RK, Mallela RK, Cornuet PK, et al. Characterization of Three-Dimensional Retinal Tissue Derived from Human Embryonic Stem Cells in Adherent Monolayer Cultures. Stem Cells Dev. 2015;24(23):2778-95.
21. Chen G, Gulbranson DR, Hou Z, et al. Chemically defined conditions for human iPSC derivation and culture. Nat. Methods 2011;8(5):424–429.
22. Vaajasaari H, Ilmarinen T, Juuti-Uusitalo K, et al. Toward the defined and xeno-free differentiation of functional human pluripotent stem cell-derived retinal pigment epithelial cells. Mol. Vis. 2011;17:558–75.
23. Pennington BO, Clegg DO, Melkoumian ZK, et al. Defined culture of human embryonic stem cells and xeno-free derivation of retinal pigmented epithelial cells on a novel,

synthetic substrate. Stem Cells Transl. Med. 2015;4(2):165–77.

24. Plaza Reyes A, Petrus-Reurer S, Antonsson L, et al. Xeno-Free and Defined Human Embryonic Stem Cell-Derived Retinal Pigment Epithelial Cells Functionally Integrate in a Large-Eyed Preclinical Model. Stem Cell Reports 2015;6:1–9.
25. Schwartz SD, Tan G, Hosseini H, et al. Subretinal Transplantation of Embryonic Stem Cell-Derived Retinal Pigment Epithelium for the Treatment of Macular Degeneration: An Assessment at 4 Years. Invest. Ophthalmol. Vis. Sci. 2016;57(5):ORSFc1-9.
26. Tucker BA, Anfinson KR, Mullins RF, et al. Use of a synthetic xeno-free culture substrate for induced pluripotent stem cell induction and retinal differentiation. Stem Cells Transl. Med. 2013;2(1):16–24.
27. Sridhar A, Steward MM, Meyer JS. Nonxenogeneic growth and retinal differentiation of human induced pluripotent stem cells. Stem Cells Transl. Med. 2013;2(4):255–64.
28. Reichman S, Goureau O. Production of Retinal Cells from Confluent Human iPS Cells. Methods Mol. Biol. 2016;1357:339-51.
29. Belle M, Godefroy D, Dominici C, et al. A Simple Method for 3D Analysis of Immunolabeled Axonal Tracts in a Transparent Nervous System. Cell Rep. 2014;9(4):1191–1201.
30. Fuhrmann S. Eye morphogenesis and patterning of the optic vesicle. Curr. Top. Dev. Biol. 2010;93:61–84.
31. Mathers PH, Jamrich M. Regulation of eye formation by the Rx and pax6 homeobox genes. Cell. Mol. Life Sci. 2000;57(2):186–94.
32. MacLaren RE, Pearson RA, MacNeil A, et al. Retinal repair by transplantation of photoreceptor precursors. Nature 2006;444(7116):203–7.
33. Barber AC, Hippert C, Duran Y, et al. Repair of the degenerate retina by photoreceptor transplantation. Proc. Natl. Acad. Sci. U. S. A. 2013;110(1):354–9.
34. Lakowski J, Han Y-T, Pearson RA, et al. Effective transplantation of photoreceptor precursor cells selected via cell surface antigen expression. Stem Cells 2011;29(9):1391–404.

35. Eberle D, Schubert S, Postel K, et al. Increased integration of transplanted CD73-positive photoreceptor precursors into adult mouse retina. Invest. Ophthalmol. Vis. Sci. 2011;52(9):6462–71.

36. Ferreira TS, Postel K, Stutzki H, et al. Daylight Vision Repair by Cell Transplantation. 2014;(1):1–15.

37. Finnemann SC, Bonilha VL, Marmorstein AD, et al. Phagocytosis of rod outer segments by retinal pigment epithelial cells requires alpha(v)beta5 integrin for binding but not for internalization. Proc. Natl. Acad. Sci. U. S. A. 1997;94(24):12932–7.

38. Nandrot EF, Anand M, Almeida D, et al. Essential role for MFG-E8 as ligand for alphavbeta5 integrin in diurnal retinal phagocytosis. Proc. Natl. Acad. Sci. U. S. A. 2007;104(29):12005–12010.

39. Hollenberg MJ, Spira AW. Human retinal development: Ultrastructure of the outer retina. Am. J. Anat. 1973;137(4):357–385.

40. Koso H, Minami C, Tabata Y, et al. CD73, a novel cell surface antigen that characterizes retinal photoreceptor precursor cells. Invest. Ophthalmol. Vis. Sci. 2009;50(11):5411–8.

41. Shirai H, Mandai M, Matsushita K, et al. Transplantation of human embryonic stem cell-derived retinal tissue in two primate models of retinal degeneration. Proc. Natl. Acad. Sci. 2016;113(1):201512590.

42. Kamao H, Mandai M, Okamoto S, et al. Characterization of human induced pluripotent stem cell-derived retinal pigment epithelium cell sheets aiming for clinical application. Stem Cell Reports 2014;2(2):205–218.

43. Taylor CJ, Peacock S, Chaudhry AN, et al. Synthesis Generating an iPSC Bank for HLA-Matched Tissue Transplantation Based on Known Donor and Recipient HLA Types. 2012:147–152.

44. Wilmut I, Leslie S, Martin NG, et al. Development of a global network of induced pluripotent stem cell haplobanks. Regen. Med. 2015;10(3):235–8.

Figure legends

Figure 1. Generation of retinal organoids from adherent hiPSCs in Xeno Free and Feeder Free conditions.

(A) Schematic diagram illustrating the protocol for retinal organoid production from hiPSCs. (B) RT-qPCR analysis of *DKK1* and *NOGGIN* during differentiation at D0, D14 and D28. Data are normalized to hiPSC-2 at D0. (C) Self-forming neuroretinal-like structures derived from adherent hiPSCs at D28. Scale bar = 100 µm. (D) Morphology of representative floating retinal organoids isolated at D29. Scale bars= 100 µm. (E) RT-qPCR analysis of eye-field transcription factors, *NRL*, *CRX*, *NEUROD1* and pluripotency marker *POU5F1* in retinal organoids at D28. Data are normalized to hiPSC-2 at D0. (F-G) RT-qPCR time course analysis of eye-field and retinal specific transcription factors and forebrain marker *FOXG1* in retinal organoids between D28 to D56. Data are normalized to retinal organoids at D28. (H-O) Immunostaining of retinal organoid sections at D35 for PAX6, RAX, VSX2, MITF and Ki67. Picture in panel N correspond to a transverse section of retinal organoids. Scale bars = 100 µm.

Figure 2. Photoreceptor differentiation in retinal organoids during floating cultures.

(A-B) RT-qPCR analysis of photoreceptor markers during differentiation between D35 to D175. Data are normalized to retinal organoids at D35 (A) or D56 (B). (C-N) Immunostaining of retinal organoid sections for CRX (C, E, N), OTX2 (C), CD73 (D, F, J), RECOVERIN (D-F, I, L), RHODOPSIN (G, H, K, M), R/G OPSIN (H), BLUE OPSIN (K), Acetylated TUBULIN (I) and CONE ARRESTIN (J, N) at the indicated time of differentiation. Nuclei were counterstained with DAPI (blue). Scale bars = 50 µm (C, D, G-I) or 100 µm (E, F, J-N).

Figure 3. Maturation and electrophysiological analysis of hiPSC-derived photoreceptors.

(A-D) Immunolabeling for RHODOPSIN (A-D), RECOVERIN (A, C) or CONE ARRESTIN (B) and 3DISCO clearing of D195 retinal organoids. Scale bars = 200 µm (A-C) and 25 µm (D).

(E-L) Transmission electronic microscopy analysis of retinal organoids at D112 and D196 with the presence of external limiting membrane (*), basal bodies (BB), connecting cilia (CC), centrioles (CT) mitochondria (MT), inner segments (IS) and disc stacks (DS) Photoreceptor-specific microtubule arrangements revealed the presence of the clearly identifiable 9x3+0 basal body complex BB and 9x2+0 connecting cilium (CC). Scale bars = 1 µm (E, G, H); 500 nm (F, I, L); 100 nm (J, K). (M) Calcium imaging on dissociated retinal cells at D175. Examples (Ex.1 and Ex.2) of 2-Photon Fura2-AM fluorescence images obtained before (left) and during (right) application of 8-Br-cGMP. White arrows on Ex.1 denoted 1 and 2 represent a responsive and a non-responsive cell, respectively. On Ex.2, the arrow represents another responsive cell. Fluorescent images are represented in false colors and are averages of 20 seconds of activity before or during stimulation. A cGMP-based calcium influx is reflected by a decrease in Fura2-AM fluorescence, and such a response is observed in both examples in one cell, without affecting neighbor cells. Scale bars = 5 µm. (N) Fluorescence raw traces and effect of an application of cGMP analogue on the cells 1 and 2 displayed on Ex.1, expressed as percentage change from baseline fluorescence (Δf/f %). (O) Boxplot representing the average decrease in fluorescence amplitude of 11 responsive cells from three independent samples.

Figure 4: Sequential generation of retinal ganglion cells, horizontal cells, amacrine cells, Müller glial cells and bipolar cells from floating retinal organoids.

(A) Immunofluorescence staining of cryosectioned retinal organoids at D28 for Ki67 and VSX2. (B-F) Immunohistochemical analysis of retinal organoids between D35 to D84 using markers for RGCs (BRN3A, PAX6), horizontal cells (LIM1, PAX6), amacrine cells (AP2, PAX6) and photoreceptors (OTX2). Scale bars = 100 µm. (G-J) Immunohistochemical analysis of retinal organoids after D140 using markers for proliferating cells (Ki67) and for late retinal cell types, Müller glial cells (GS, SOX9) and bipolar cells (VSX2, PKCα). Nuclei were counterstained with DAPI (blue). Scale bars = 100 µm (H, I) and 50 µm (G, J). (K-M) RT-qPCR analysis of selected neural retinal cell types in retinal organoids at different times:

RGCs (*BRN3A*, *BRN3B*); horizontal cells (*LIM*), amacrine cells (*GAD2*), Müller glial cells (*GLAST1*, *RLBP1*) and bipolar cells (*PKCα*). Data are normalized to retinal organoids at D28 (K, L) or D56 (M).

Figure 5. Efficient cryopreservation of photoreceptor precursors in whole retinal organoids or as dissociated cells.

(A-D) Immunostaining for CRX (A, B), CD73 (C, D) and RECOVERIN (A-D) on retinal organoids at D100. Scale bars = 100 µm. (E-H) Immunostaining for CRX (E, F), CD73 (G, H) and RECOVERIN (E-H) on retinal organoids cryopreserved at D84 and cultured for additional 16 days after thawing. Scale bars = 100 µm. (I-P) Retinal organoids were dissociated at D84 (I-L) or D100 (M-P) and retinal cells were either cultured for 5 days *in vitro* (DIV) (I, J, M, N) or cryopreserved and cultured for 5 DIV after thawing (K, L, O, P) before immunostaining for CD73 (I-L), CRX (M-P) and RECOVERIN (I-P). Scale bars = 100 µm (I, K, M, O) and 25 µm (J, L, N, P). (Q) Quantitative analysis at D100 of CRX-positive cells in unfrozen retinal organoids (control, *N*= 7 organoid sections corresponding to 81,450 cells) or in retinal organoids cryopreserved at D84 (*N* =11, organoid sections corresponding to 119,339 cells). (R) Quantitative analysis after 5 DIV of double CRX/RECOVERIN-positive cells in fresh (control, n=31,303 cells) or cryopreserved dissociated cell population from D100 retinal organoids (n=13,958 cells).

Figure 6. Generation and characterization of hiRPE cells in Xeno-Free and Feeder-Free conditions.

(A) Schematic diagram illustrating different steps for the generation, amplification, and storage of RPE cells from adherent culture of iPSCs. (*) Pigmented patch picking time. (B) Phase-contrast images of pigmented patches of hiRPE cells from hiPSC-2 at D42. Scale bar = 3 cm. (C-E) Phase-contrast images of hiRPE cells at passage 0 (hiRPEp0) and at passage 3 (hiRPEp3), respectively at 6 weeks (W6) after picking and at W2 or W14 after passaging. Scale bar = 100 µm. (F) MITF and ZO-1 immunostaining of hiRPEp3 cells, 2 weeks in culture

after thawing. Scale bar = 100 µm. (G, H) Z-stack confocal images showing typical polarized expression of BEST1 and ERZIN in hiRPEp3 cells. Scale bars = 10 µm. (I, J) RT-qPCR analysis of mature RPE-associated markers in hiRPEp3 cells cultured 2 (W2), 6 (W6) or 14 weeks (W14) after thawing. Data are normalized on hiRPEp3 cells at 2W. (K) Evaluation of RPE cell phagocytic activity: ratios of FITC/DAPI fluorescence were evaluated in hiRPEp3 cells, ARPE-19 cell line and fibroblasts after 3hrs of incubation with FITC-labeled POS to determine binding and uptake of POS in absence (blue bars) or in presence (red bars) of function-blocking antibody anti $\alpha v\beta 5$ integrin. Values represent the mean ± SD (*: $p<0.05$; **: $p<0.01$; ***: $p<0.005$; ****: $p<0.001$) from three separate experiments. (L-Q). Qualitative representation of internalization of FITC-labeled POS (green) by hiRPEp3, ARPE-19 and fibroblasts (nuclei counterstained in blue) in absence or in presence of the anti $\alpha v\beta 5$ integrin blocking antibody. Scale bars = 25 µm.

Graphical abstract legend

Schematic diagram illustrating the method allowing the production and the cryopreservation of retinal organoids, photoreceptor precursors and retinal pigmented epithelium in xeno and feeder free culture conditions.

Goureau, Figure 1, top

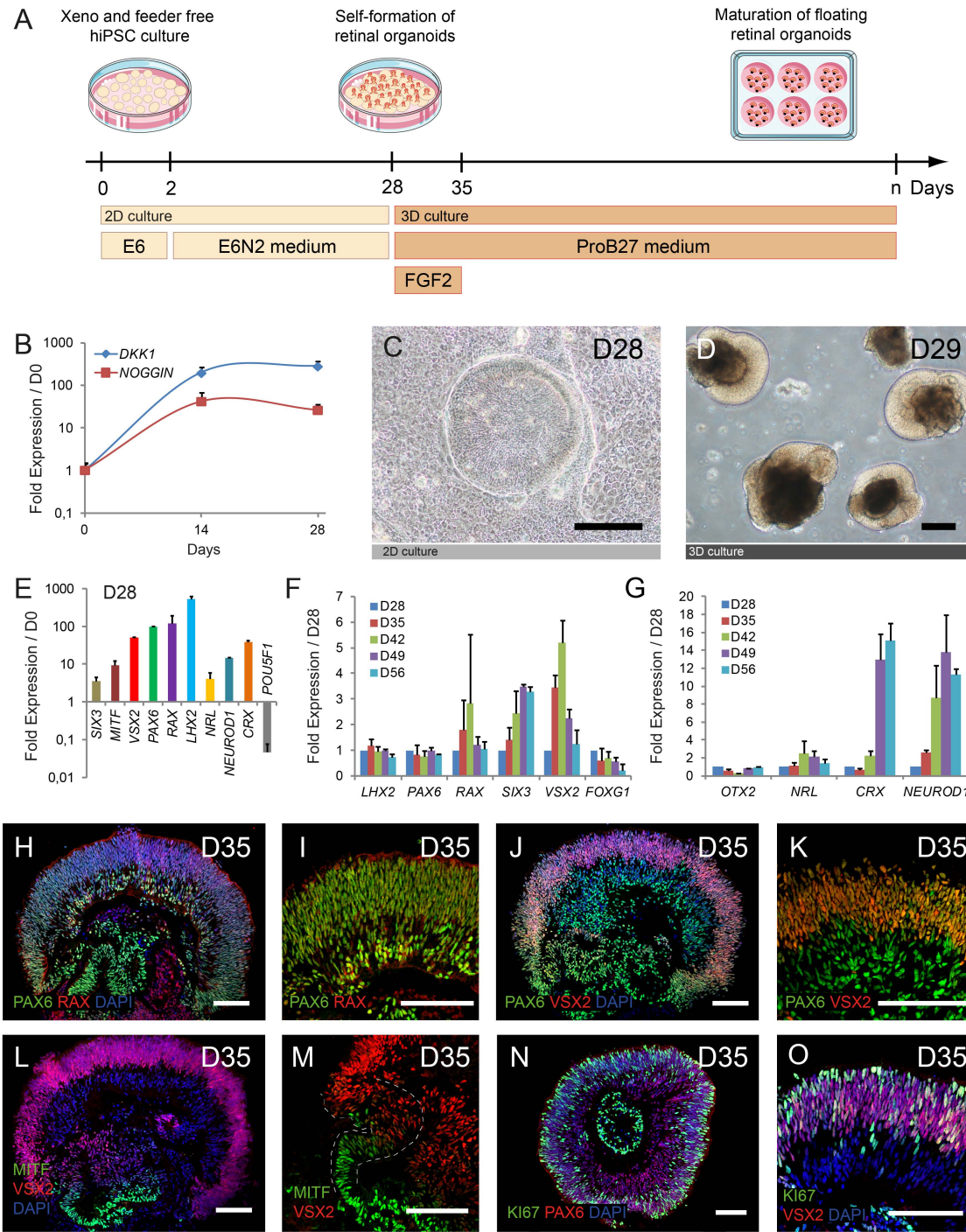

Goureau, Figure 2, top

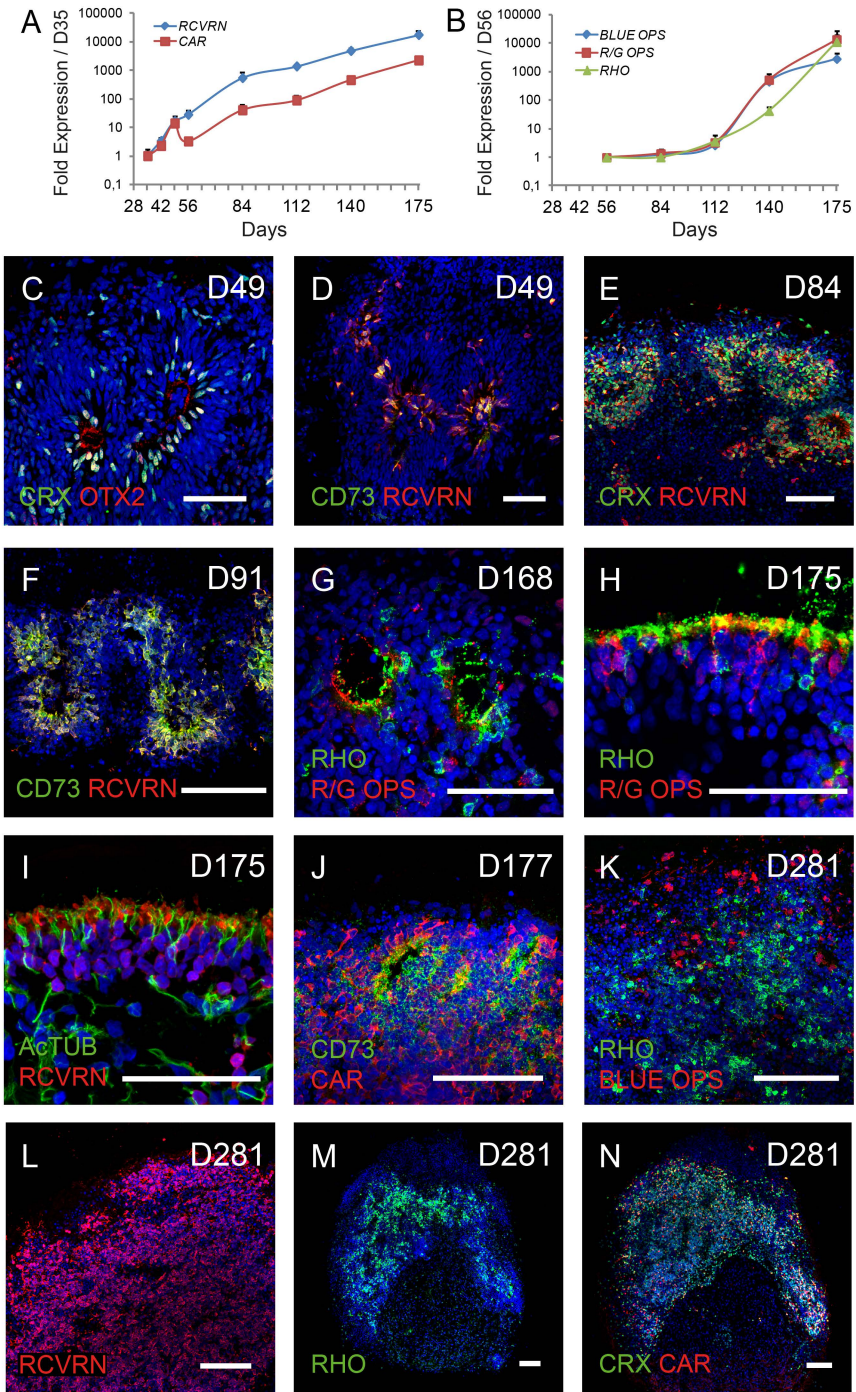

Goureau, Figure 3, top

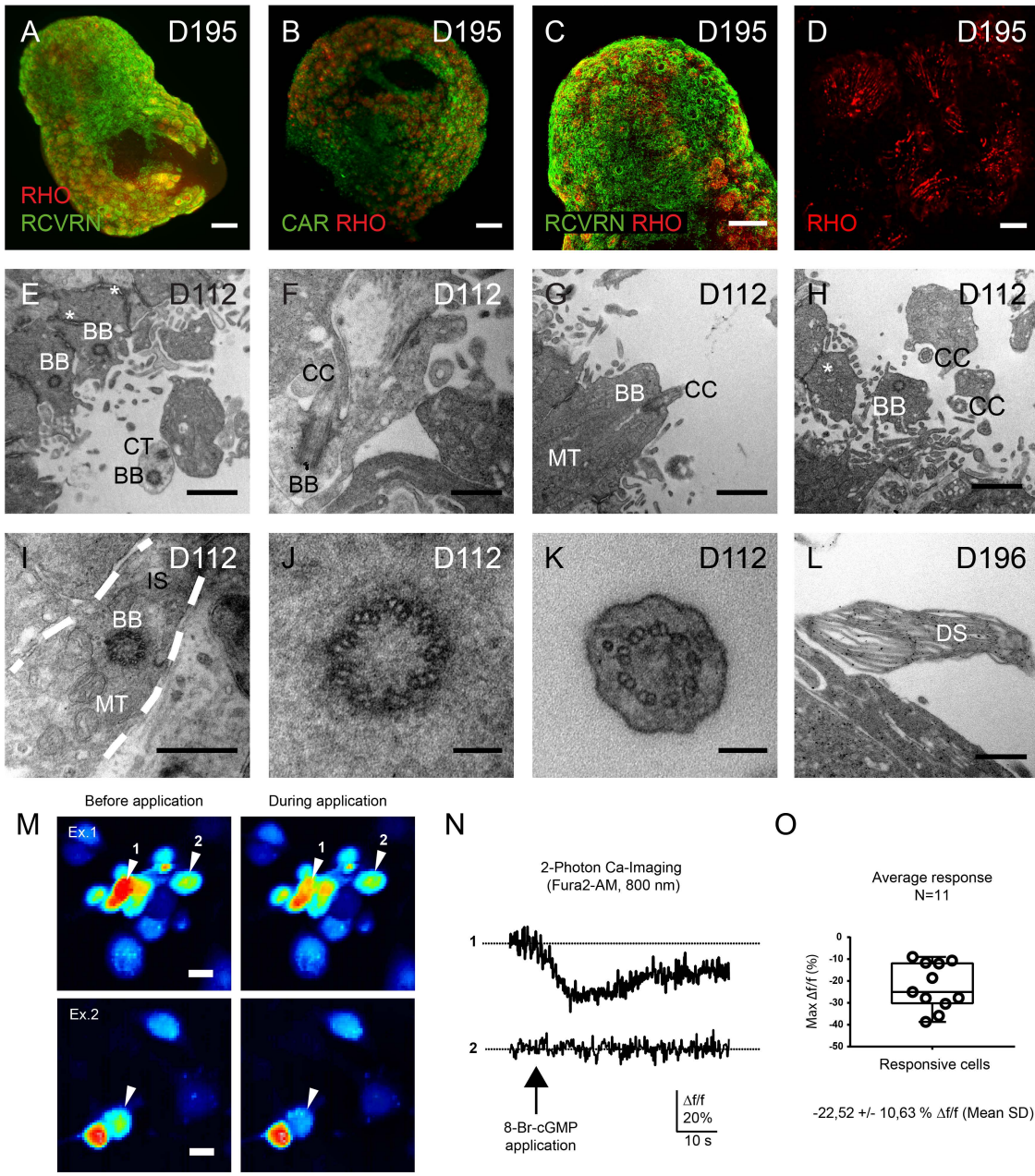

Goureau, Figure 4, top

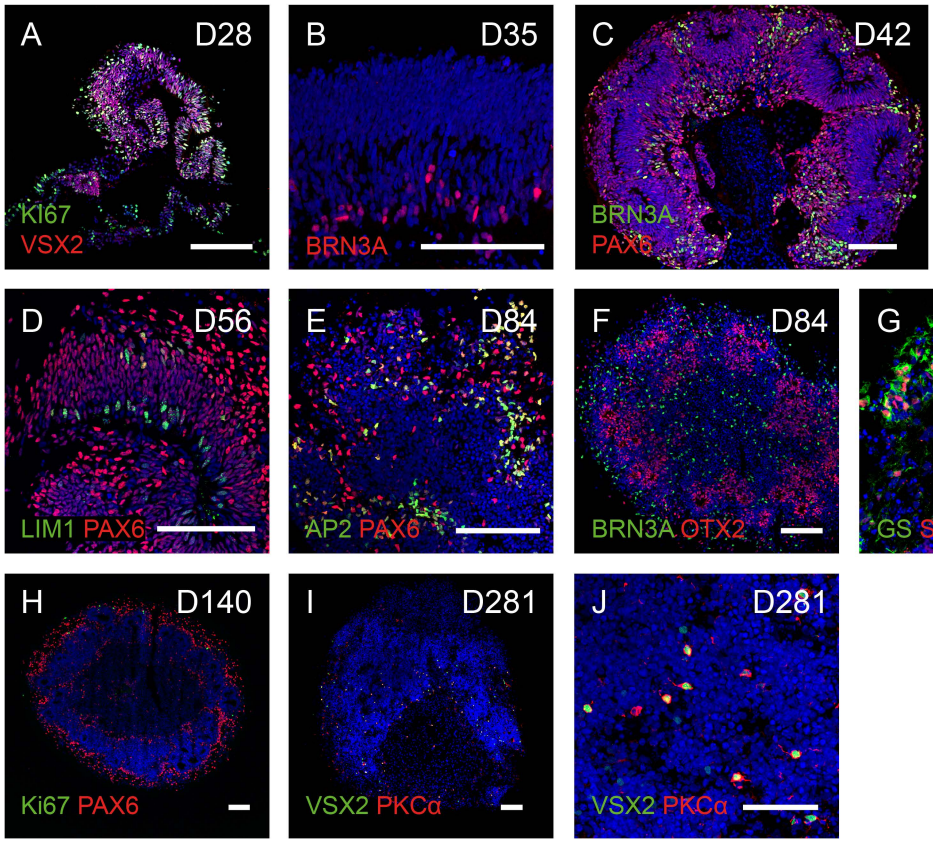

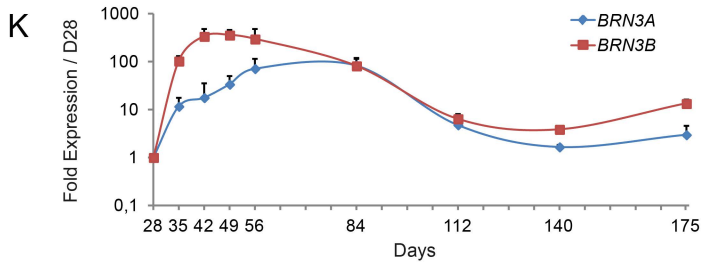

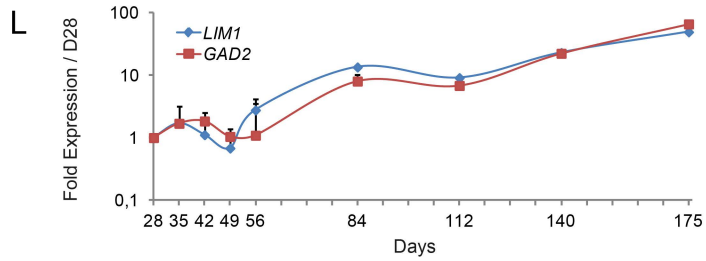

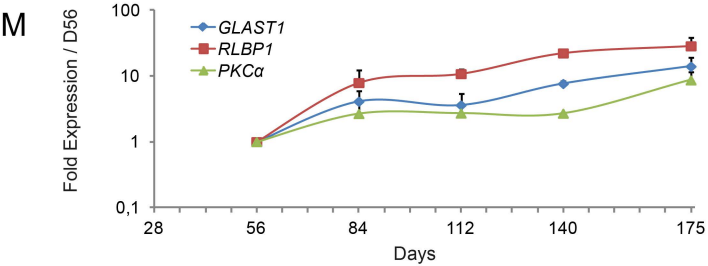

Goureau, Figure 5, top

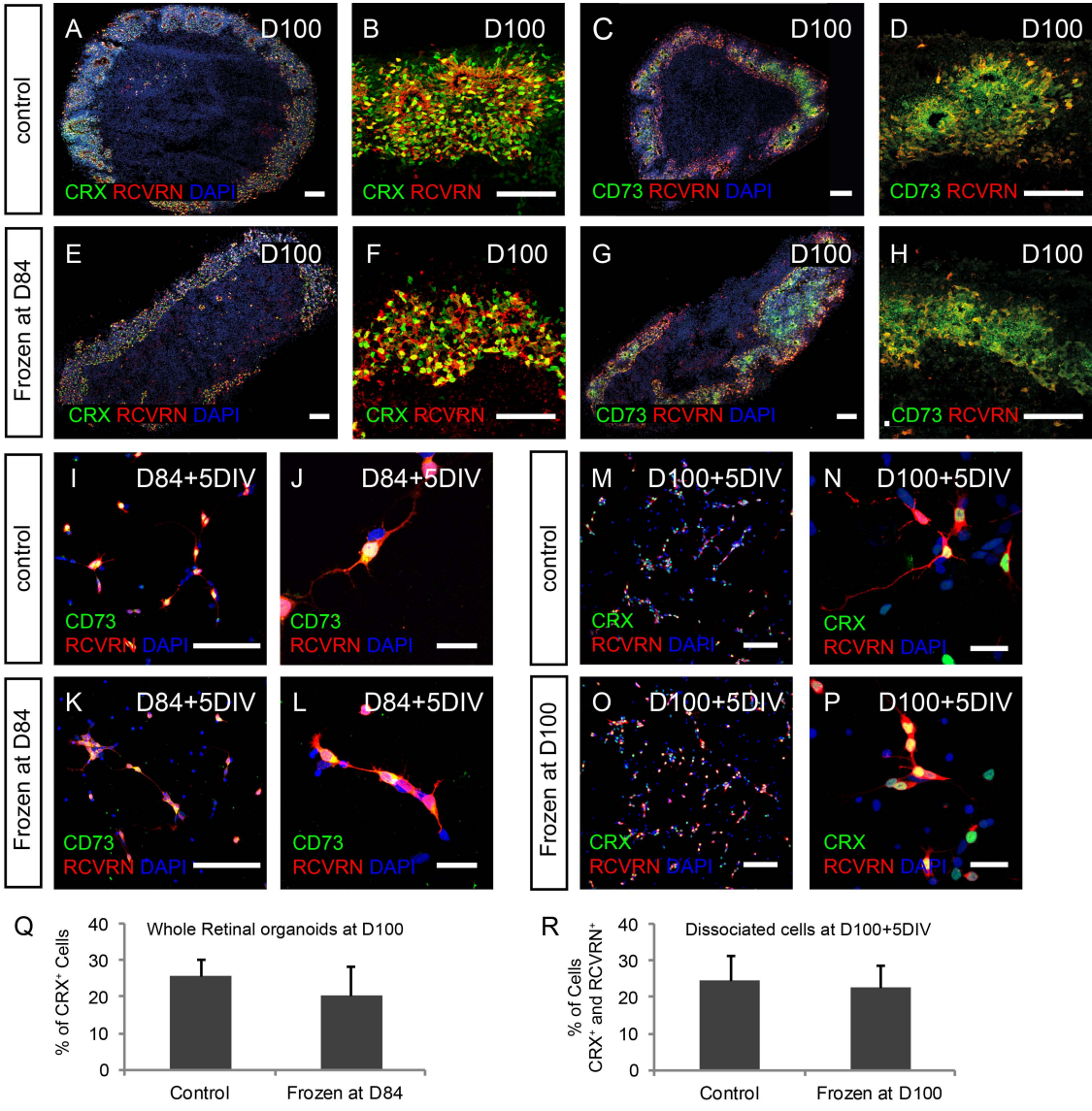

Goureau, Figure 6, top